

Phase stability and the equation of state of FeS at high pressures and temperatures

A. Kavner[‡], T.S. Duffy[†], and G. Shen[‡]

[†]Department of Geosciences, Princeton University, Princeton, NJ 08544 USA

[‡]GSECARS, University of Chicago, Chicago, IL 60637 USA

Introduction

Understanding a planet's structure and evolution requires combining geophysical evidence (e.g., seismology and gravitational observations) with mineralogical measurements of candidate materials at relevant conditions of planetary interiors. Iron alloys are believed to be the principal constituent of terrestrial planets' cores, and sulfur is a likely candidate for a major alloying component. Recent advances in our understanding of Martian geophysics and the possibility for future seismological exploration there have spurred our interest in measuring the high-pressure, high-temperature behavior of stoichiometric iron sulfide at the conditions of the Martian core.

Iron sulfide is also interesting from a materials science perspective. It undergoes a series of structural and electronic phase transformations as pressure and temperature are increased, including a semiconductor-to-metal transformation [1]. A pressure vs. temperature (P-T) phase diagram for FeS is shown in Figure 1. There are still uncertainties about the exact structures of the high-pressure FeS phases and of the nature about the electronic transitions.

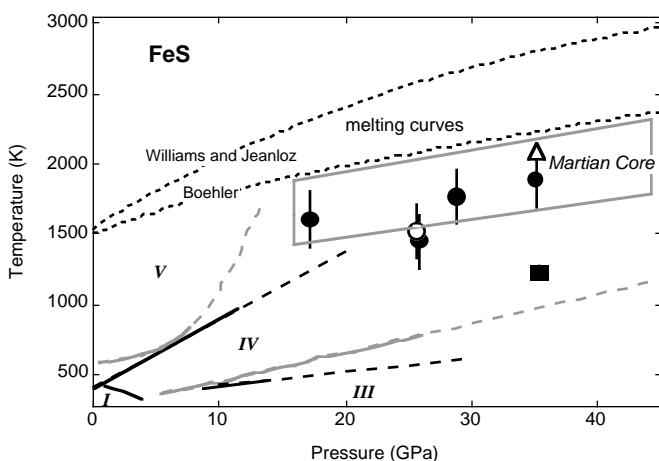


Figure 1: P-T phase diagram of FeS. Solid circles indicate the presence of (a,c) hexagonal FeS(V), while the open circle shows (2a, c) FeS(IV). Filled square indicates the highest temperature at which FeS(III) is observed. The open triangle indicates FeS melting. Lower P-T phase boundaries are shown as gray [2] and black [5]; dashed lines represent the authors' extrapolations. Experimentally determined melting curves of FeS are shown [7, 8]. Plausible temperature ranges for the Martian core are also shown.

Methods and Materials

All experiments were performed at the GSECARS sector of the Advanced Photon Source (APS) at Argonne National Laboratory (ANL). The starting material is a synthetic,

stoichiometric FeS sample synthesized by Fei [2]. A foil of FeS was loaded into a symmetric diamond anvil cell, sandwiched between two layers of MgO to thermally insulate the sample from the diamond surfaces, and also to serve as a pressure proxy. The FeS sample was heated using a double-sided Nd:YLF laser-heating system, as described by Mao, *et al.* [3]. Thermal radiation was collected from both sides of the sample surface, dispersed by an imaging spectrometer, and the intensity (as a function of wavelength) was measured on a CCD. Temperature was determined by fitting the spectral intensity, corrected for the system response, to Wien's approximation to Planck's law. Temperature as function of distance across the hotspot was determined for the FeS sample *in situ*.

Energy-dispersive x-ray diffraction patterns, using a fixed angle of $2\theta = 5.5^\circ$, were taken throughout the heating cycles. Special care was taken to ensure the alignment of the laser hotspot with the central part of the x-ray beam. The sample was also visually monitored during heating using remote cameras focused on each side of the sample. Five heating cycles were performed on two separate samples of FeS. The pressure was determined by referencing the 100% diffraction peak (200) of MgO to a nonhydrostatic room-temperature MgO equation of state ($K_{OT} = 177$ GPa, $K_{OT}' = 4$ GPa) [4].

Results and Discussion

The heating cycle at 35 GPa (Figure 2) shows the presence of two phase transformations in FeS. At the peak temperature, visual observation of the FeS revealed rapid textural changes indicative of fluid flow associated with melting. The corresponding diffraction pattern showed only peaks due to the MgO insulation layer. As the sample temperature was lowered, peaks indicating the presence of hexagonal FeS appeared, including the (200), (002), and (201) triplet. The appearance of hexagonal FeS under cooling conditions suggested that the crystals nucleated from the FeS melt, providing a strong confirmation of the thermodynamic stability of the hexagonal phase at these conditions. As the sample temperature was lowered further, the hexagonal peaks disappeared and were replaced by diffraction lines consistent with FeS(III) [2, 5, 6]. The 300 K diffraction patterns both before and after heating are also consistent with the presence of FeS(III).

This data set, thus, constrains the FeS melting point and monoclinic-hexagonal transformation at 35 GPa to be 2100(100) K and 1225(25) K, respectively (Figure 1). The former is consistent with the melting curve reported by Boehler [7], while the latter indicates that phase III persists to higher temperatures than expected based on extrapolation of low P-T data [2, 5].

The high-temperature diffraction patterns for each of the heating cycles reveal the presence of hexagonal FeS throughout the conditions of the Martian core (Figure 3). All but one of the integrated patterns can be indexed as the NiAs structure [FeS(V)]. The pattern at 23 GPa showed evidence of the superlattice peak (001) corresponding to the distorted NiAs cell [FeS(IV)]. This indicates that the FeS(IV)-FeS(V) phase boundary will cross the range of predicted P-T conditions of the Martian interior (Figure 1), ruling out a previous suggestion [2] that FeS in the Martian core would be wholly in the stability field of phase IV; our result is consistent with extrapolation of the IV-V boundary from another low P-T study [5].

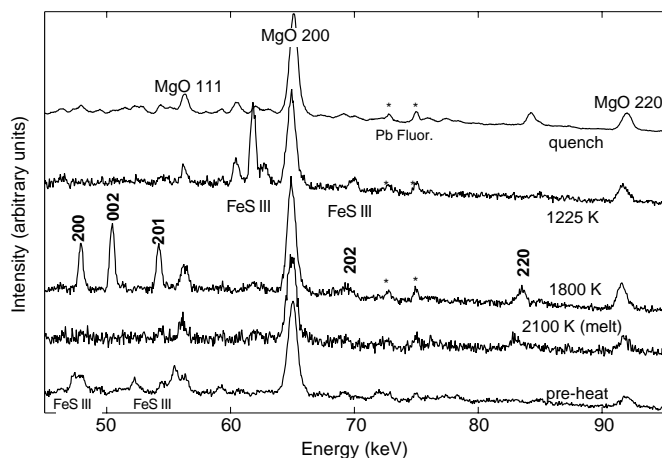


Figure 2: Diffraction patterns from FeS heating cycle at 35 GPa. The average temperature is indicated alongside each pattern. MgO, hexagonal FeS, and fluorescence lines are labeled. The lower temperature diffraction patterns are not indexed, but are compatible with the presence of monoclinic FeS phase III.

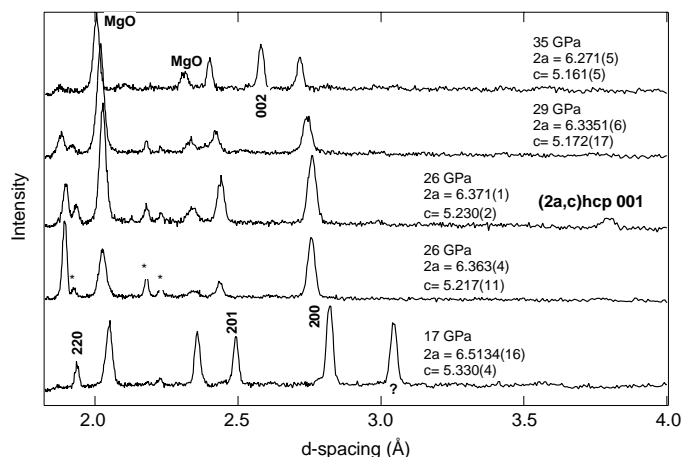


Figure 3: High-temperature diffraction patterns for each heating cycle plotted as a function of d-spacing. (*) indicates Pb fluorescence peaks. The hexagonal unit cell parameters are shown above each diffraction pattern.

Acknowledgments

We thank Y. Fei for providing sample material and for useful discussions. We also thank W. Panero and S. Shim for experimental assistance and more useful discussions. Portions of this work were performed at GeoSoilEnviroCARS (GSECARS), sector 13, APS at Argonne National Laboratory. GSECARS is supported by the National Science Foundation - Earth Sciences, Department of Energy - Geosciences, W. M. Keck Foundation, and the United States Department of Agriculture. Use of the Advanced Photon Source was supported by the U. S. Department of Energy, Basic Energy Sciences, Office of Energy Research, under Contract No. W-31-109-Eng-38.

References

- [1] H.K. Mao, G. Zou, and P.M. Bell, *Carnegie Institution of Washington Yearbook* **80**, 267 (1981).
- [2] Y. Fei, C.T. Prewitt, H-k. Mao, and C.M. Bertka, *Science* **268**, 1892 (1995).
- [3] H-k. Mao, G. Shen, R.J. Hemley, and T.S. Duffy, in *Properties of Earth and Planetary Materials at High Pressure and Temperature*, (Geophysical Monograph 101, AGU 1998).
- [4] T.S. Duffy, R.J. Hemley, and H.-k. Mao, *Phys. Rev. Lett.* **74**, 1371 (1995).
- [5] K. Kusaba, Y. Syono, T. Kikegawa, and O. Shimomura, *J. Phys. Chem. Sol.* **59**, 945–950 (1998).
- [6] R.J. Nelmes, M.I. McMahon, S.A. Belmonte, and J. B. Parise, *Phys. Rev. B* **59**, 9048–9052 (1999).
- [7] R. Boehler, *Earth Plan. Sci. Lett.* **111** 217–227 (1992).
- [8] Q. Williams and R. Jeanloz, *J. Geophys. Res.* **95**(19), 299–310 (1990).